

## An Improved Three-dimensional MIMO channel Model based on GBSBEM

Ming LI\* and Yun-fei GUO

National Digital Switching System Engineering & Technological Research Center,  
Zhengzhou, Henan province, 450002, China

Received 20 June 2013; Accepted 23 December 2013

### Abstract

Geometrically based single-bounce elliptical model (GBSBEM) does not consider the impact of time delay and pitch angle, and cannot response the correlation between MIMO antennas. In order to solve these problems, an improved three-dimensional MIMO channel model based on GBSBEM is presented. By introducing spatial distance and pitch angle, this model transformed the 2D GBSBEM to 3D GBSBEM, which includes space distance, direction of arrival (AOA) and multipath time delay. And the probability density functions of the AOA, time delay and their joint are also derived. What's more, by building 3D GBSBEM between multi-antennas, 3D MIMO GBSBEM is presented. For illustration, MATLAB simulation is utilized to show the feasibility and applicability of this 3D MIMO GBSBEM. The analysis results show that the improved model is not only compatible with the original model, but also improve the accuracy of the latter, and extend the scope of its application. The improved model is more suitable for analyzing the signal reception performance of MIMO communication systems.

*Keywords:* MIMO channel model, GBSBEM, AOA, Pitch angle

### 1. Introduction

In MIMO wireless fading channel, the direction of wave propagation is directional and non-uniformity. However, the wider application of MIMO channel model based on the direction and angle geometric statistical properties are built under an ideal condition that transmitting antennas and receiving antennas are located in the same horizontal plane. Therefore, geometrically based scatter (GBS) model is not fit for establishing MIMO channel models. GBS model can realize a concise description of the radio channel, and does not require extensive and time-consuming measurement for analyzing the channel characteristics, such as geometrically based single-bounce elliptical model (GBSBEM)<sup>[1]</sup> and geometrically based single-bounce circle model (GBSBCM)<sup>[2]</sup>. In order to make the GBS model suitable for MIMO channel modeling, a lot of literature research MIMO channel of GBS models. In literature [3], Lee model assumed scatters uniformly distributed in a ring around the mobile station. Literature [4] assumed that N scattering bodies in the range of the angle of AOA. All of these literatures used different functions to describe the distribution of the channel angle and scattering bodies. However, these models did not consider the impact of time delay. For this reason, the space time frequency correlation function of MIMO channel cannot be expressed.

Literature [5] has confirmed that the scattering signals in radio channel have large pitch angles. So researches for

MIMO channel must consider the influences of pitch angle and time delay, and need to create a three-dimensional model. Literature [6], referring [5], built a 3D GBS model, but assumed that received signals at the receiver were evenly distributed in the range of angular spread. Literature [7] created a three-dimensional channel model for different receiver arrays, considering the influence of pitch angle, but assuming the horizontal angle and the pitch angle were uniformly distributed.

To solve this problem, an improved 3D-MIMO-GBSBEM is presented in this research. This model introduces space distance vector, AOA and time delay as the model parameters, and derive the probability density functions of the AOA, and the space time frequency correlation function of MIMO channel. MATLAB simulation results show that the improved 3D-MIMO-GBSBEM model is not only compatible with the traditional GBSBEM, but also overcome the limitations of the latter. This model can be used more widely in MIMO channel modeling by selecting appropriate parameter settings.

### 2. The Improved 3D-GBSBEM

#### 2.1 model of 3D-GBSBEM

As shown in Fig.1, Tx, Rx, are the transmitting antenna and receiving antenna respectively. Many ellipses with different lengths characteristics can be obtained using Tx and Rx as focus. A, B and C are random scattering points in these ellipses. Elliptical model depicted in this manner has two characteristics:

\* E-mail address: dingdli@gmail.com

- (1) although the distance between A and Rx is different to the distance between B and Rx, A and B have the same angle of arrival. So they have same Doppler frequency;
- (2) according to the nature of ellipse, A and C are in the same ellipse, and they have the same path length. So they have the same propagation delay.

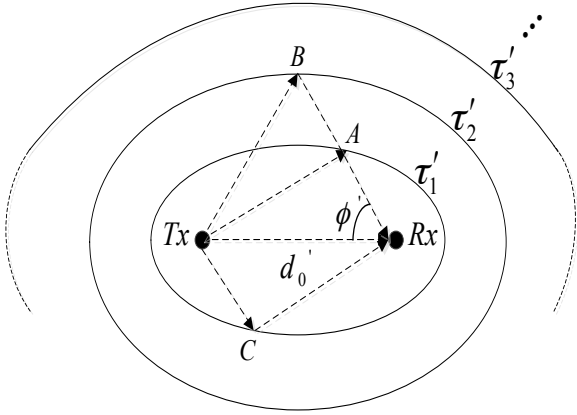


Fig. 1. an GBSBEM channel model

Elliptic equations is defined as:

$$\frac{x^2}{a^2} + \frac{y^2}{b^2} = 1 \quad (1)$$

Where

$$a = c\tau_i / 2$$

$$b = \sqrt{a^2 - f^2}$$

$$f = d_0 / 2$$

C is speed of light, and  $\tau_i$  is time delay.

Based on the GBSBEM, AOA's probability density function on the standard time delay is defined as:

$$f(\phi | \tau_i) = \frac{(\tau_i^2 - 1)^{3/2} (\tau_i^2 - 2\tau_i \cos \phi + 1)}{\pi(2\tau_i^2 - 1)(\tau_i^2 - \cos \phi)^3} \quad -\pi < \phi < \pi \quad (2)$$

It can be seen that original GBSBEM does not consider the pitch angle formed by the transmitting antenna, receiving antenna and the horizontal plane. When communication distance is far away, the pitch angle is very small, and the time delay is long. While communication is taken place between the high-rise buildings in an urban environment, the pitch angle is larger, and the time delay is smaller compared with long distance communication. In this way, original two-dimensional GBSBEM established under the horizontal will no longer be able to guarantee its accuracy.

In order to make up for the deficiencies of the original 2D-GBSBEM, a new improved ellipsoid model is constructed within a three-dimensional coordinate system. This model makes the transmitting antenna and the receiving antenna as the ellipsoid's focuses. What's more, it assumes that the scattering signals reached the receiving antenna have

experienced only one reflection, and scattering bodies are uniformly distributed in the ellipsoid.

Its cross-sectional view is shown in Fig. 2:

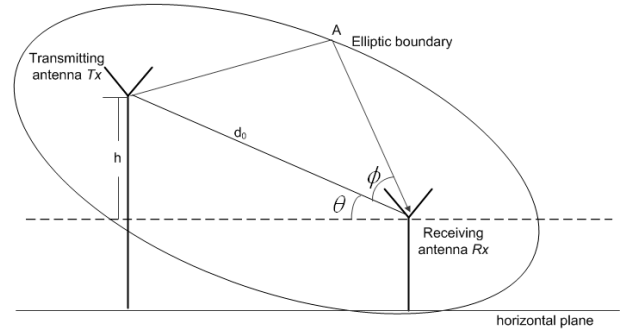


Fig. 2. sectional view of the 3D-GBSBEM

Where

$d_0$  is the distance between transmitting antenna Tx and receiving antenna Rx.

$\tau_0$  is the smallest absolute delay,  $\tau_0 = d_0 / c$

$\theta$  is the pitch angle formed by the transmitting antenna, receiving antenna and the horizontal surface.

A is assumed as an arbitrary point on the elliptical boundary, which its time delay is  $\tau_i$ .

$\phi$  is AOA, and  $\phi = \angle AR_x T_x$ .

$r_i$  is standard delay, and  $r_i = \tau_i / \tau_0$

## 2.2 The PDF of AOA

According to the nature of ellipsoid, a three-dimensional elliptic equations is built as follows:

$$\frac{(z - z_0)^2}{a^2} + \frac{x^2}{b^2} + \frac{y^2}{b^2} = 1 \quad (3)$$

Where,  $z_0$  is an offset in the Z-axis of ellipsoid.

In order to facilitate the analysis, this 3D-GBSBEM model is mapped to horizontal plane. The mapped equation is:

$$\frac{(x - f_0)^2}{a_0^2} + \frac{y^2}{b_0^2} = 1 \quad (4)$$

This equation's parameters are defined as follows:

$$a_0 = \frac{ab^2}{a^2 \sin^2 \theta + b^2 \cos^2 \theta}$$

$$b_0 = \frac{b^2}{\sqrt{a^2 \sin^2 \theta + b^2 \cos^2 \theta}}$$

$$f_0 = \frac{b^2 \sqrt{a^2 - b^2} \cos \theta}{a^2 \sin^2 \theta + b^2 \cos^2 \theta}$$

According to this mapped equation, the relationship between the AOA and the mapped standard time delay in horizontal plane can be obtained. The relationship is shown as:

$$\phi = \arccos \frac{r_{i0}}{2r_i^2 - 1} \quad (5)$$

Where  $r_{i0}$  is assumed the standard time delay in horizontal plane,  $r_{i0} = r_i / \cos \theta$ .

In order to generate the probability density function of AOA, this research uses the distribution function method, and obtains the AOA's conditional probability density function according to the formula (3), (4) and (5), shown as follows:

$$f(\phi|r_i) = \frac{(r_i^2 - 2r_i \cos \phi \cos \theta + \cos^2 \theta)(r_i^2 - \cos^2 \theta)^{3/2}}{\pi(2r_i^2 - \cos^2 \theta)(r_i - \cos \phi \cos \theta)^3}, -\pi < \phi < \pi \quad (6)$$

### 2.3 The PDF of standard time delay

It was found that the delay can be approximated by an exponential distribution [8] in distance environment, such as the close scattering bodies, tall buildings and mountains, by analyzing the measured environmental in literature [8] and [9]. Therefore, the 3D-GBSBEM proposed in this study, also believes that scattering bodies obey the uniform distribution on the ellipse in the same delay. At the same time, these scattering bodies obey exponential distribution on the ellipse in the different delay. Under this condition, the probability density function of the standard time delay is

$$f_r(r) = \frac{\tau_0}{\sigma} e^{-\frac{\tau_0(r/\cos\theta-1)}{\sigma}}, 1 < r < r_m \quad (7)$$

For each scattering body, the angular distribution and the distance distribution are independent, so according to the formula (6) and (7), the joint probability density function of AOA and standard time delay can be expressed as:

$$f(\phi, r_i) = f(\phi|r_i)f(r_i) = \frac{(r_i^2 - 2r_i \cos \phi \cos \theta + \cos^2 \theta)(r_i^2 - \cos^2 \theta)^{3/2} \tau_0 e^{-\frac{\tau_0(r_i - \cos \theta)}{\sigma \cos \theta}}}{\pi \sigma (2r_i^2 - \cos^2 \theta)(r_i - \cos \phi \cos \theta)^3} \quad (8)$$

## 3. The 3D-MIMO-GBSBEM

### 3.1 channel model based on 3D-MIMO-GBSBEM

Based on the 3D-GBSBEM, 3D-MIMO-GBSBEM is presented in this chapter. In Fig.3, we show the model of 3D-MIMO-GBSBEM.

Where p, q are transmitting antennas.  $S_{pq}$  is the distance between them. The m, n are receiving antennas.  $S_{mn}$  is the distance between them. The k is a random scatter in ellipsoid. Based on the k,  $\phi_{pm,k}$  is the DOA between the transmitting antenna p and the receiving antenna n. D is the horizontal distance between the transmitting and receiving antennas.

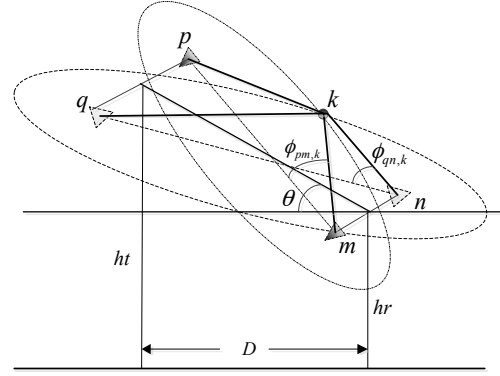


Fig. 3. MIMO model based on 3D-MIMO-GBSBEM

Assuming there is no line of sight between the transmitting antenna and receiving antenna, the channel impulse response between the transmitting antenna p and the receiving antenna m is expressed as follow:

$$h_{pm}^{NLOS}(t, \tau) = \lim_{K \rightarrow \infty} \sum_{i=1}^{N_R} \sum_{j=1}^{N_T} \sum_{k=1}^K \sum_{l=1}^L g_{k,l}^{ij} (d_{pk}^i \times d_{km}^j)^{-w_{pathloss}/2} \times \exp[j\phi_l - j \frac{2\pi}{\lambda} (d_{pk}^i + d_{km}^j)] \delta(\tau - \tau_{kl}^{ij}) \quad (9)$$

Where  $w_{pathloss}$  is the factor of path loss.  $\tau_{kl}^{ij}$  is the  $l$ th path time delay, which derived by the wave going through the scatter k.  $g_k, \phi_k$  are the random gain and random phase introduced by random scatter k. What's more,  $\{g_k^{ij}\}_{k=1}^{\infty}$  can be seen as independent and identically distributed random variables. And it's normalized form is shown as follow:

$$\lim_{K \rightarrow \infty} \frac{1}{K} \sum_{i=1}^{N_R} \sum_{j=1}^{N_T} \sum_{k=1}^K E[(g_k^{ij})^2] = 1 \quad (10)$$

### 3.2 space time frequency correlation function

Wireless fading channel second-order statistical properties can reflect the basic characteristics of the channel. It is necessary to analyze the MIMO channel spatial correlation properties in the time domain and frequency domain. The literature [3] improved the GBSBEM, but failed to give effective expression of space-time-frequency correlation function. By taking the cross-correlation of the antennas Tp-Rm and Tq-Rn shown in Fig. 3 as example, the space-time-frequency correlation function of 3D-MIMO-GBSBEM is derived and analyzed in this paper.

Space-time-frequency correlation function is defined as:

$$\rho_{pm,qn}(t, \tau) = \frac{E[h_{pm}(t)h_{qn}^*(t-\tau)]}{\sqrt{\Omega_{pm}\Omega_{qn}}} \quad (11)$$

Where  $(\bullet)^*$  means solving complex conjugate.

Assuming the waves received by different antennas have the same average power,  $\Omega_{pm} = \Omega_{qn} = \Omega$ , and the rice factors on different channels are the same,

$K_{pm} = K_{qn} = K_{Rice}$ . Based on the formula (9), and (11), Space time frequency correlation function of 3D-MIMO-GBSBEM is obtained:

$$\rho_{pm,qn}^{NLOS}(t, t-\tau, \xi, \xi-\Delta\xi) = \frac{\Omega^{-1}}{1+K_{Rice}} \lim_{K \rightarrow \infty} \sum_{l=1}^{N_n} \sum_{k=1}^{N_r} \sum_{l=1}^L E[(g_{kl}^{ij})^2] \times (d_{pk}^i \times d_{km}^j)^{-w_{pathloss}/2} (d_{qk}^i \times d_{kn}^j)^{-w_{pathloss}/2} \times \exp[j(\phi_{pm} - \phi_{qn}) - j\frac{2\pi}{\lambda}(d_{pk}^i + d_{km}^j - d_{qk}^i - d_{kn}^j)]\delta(\tau - \tau_{kl}^{ij})\delta(\Delta\xi) \quad (12)$$

When  $K \rightarrow \infty$ ,  $\frac{1}{KL} \sum_{k=1}^K \sum_{l=1}^L E[(g_{kl}^{ij})^2]$  can be approximated as  $f(\phi|r)f(r)d\phi dr$ , which is obtained in formula(8). Then the formula(12) can be simplified as follow:

$$\rho_{pm,qn}^{NLOS}(t, t-\tau, \xi, \xi-\Delta\xi) = \frac{\Omega^{-1}}{1+K_{Rice}} \iint f(\phi|\tau)f(\tau) \times (d_{pk}^i \times d_{km}^j)^{-w_{pathloss}/2} (d_{qk}^i \times d_{kn}^j)^{-w_{pathloss}/2} \times \exp[j(\phi_{pm} - \phi_{qn}) - j\frac{2\pi}{\lambda}(d_{pk}^i + d_{km}^j - d_{qk}^i - d_{kn}^j)]\delta(\Delta\xi)d\phi d\tau = S_h(\tau, \xi)\delta(\Delta\xi) \quad (13)$$

Where  $S_h(\tau, \xi)$  is the delay power spectrum density function.  $\tau$  is path delay, and  $\xi$  is time difference.

According to the characteristics of GBSBEM, the received waves transmit distance can be written as:

$$d_{pk} + d_{km} - d_{qk} - d_{kn} = (\tau_{pkm} - \tau_{qkn})c = \xi_k c$$

Since the transmit and receive antennas distance is much larger than the antenna space, the path loss can be equivalent to the form:

$$(d_{pk}^i \times d_{km}^j)^{-w_{pathloss}/2} (d_{qk}^i \times d_{kn}^j)^{-w_{pathloss}/2} = (d_{tk} \times d_{kr})^{-w_{pathloss}}$$

In this way, the delay power spectrum density function can be simplified as follow:

$$S_h(\tau, \xi) = \frac{\Omega^{-1}}{1+K_{Rice}} \iint f(\phi|\tau)f(\tau) \times (d_{tk} \times d_{kr})^{-w_{pathloss}} \times \exp[-j2\pi f \xi_k]\delta(\xi - \xi_k)d\phi d\tau \quad (14)$$

According to the channel features under the condition of wide sense stationary uncorrelated scattering (WSSUS)<sup>[4]</sup>, many other MIMO channel parameters can also be derived. For example, when  $\xi = 0$ , the delay power spectrum density function,  $S_h(\tau, \xi)$ , can also be called the delay power spectral density  $S_\tau(\tau)$ , which determines the average power of the scattered components associated with the propagation delay  $\tau$ . It can be seen that the delay power spectral density is proportional to the probability density function of propagation delay. By the delay power spectral

density, average delay and delay spread can be derived. The solving equation can be written as follows.

(a) The average delay:

$$B_\tau^{(1)} = \frac{\int_{-\infty}^{+\infty} \tau S_\tau(\tau) d\tau}{\int_{-\infty}^{+\infty} S_\tau(\tau) d\tau} \quad (15)$$

The average delay is the statistical average delay of carrier signals transmitted in multipath fading channel, and is determined by first-order of  $S_\tau(\tau)$ .

(b) The delay spread:

$$B_\tau^{(2)} = \sqrt{\frac{\int_{-\infty}^{+\infty} (\tau - B_\tau^{(1)})^2 S_\tau(\tau) d\tau}{\int_{-\infty}^{+\infty} S_\tau(\tau) d\tau}} \quad (16)$$

The delay spread, which is determined by the second-order of  $S_\tau(\tau)$ , can be used to measure the time delay of pulse going through the multipath fading channel.

Since the time-frequency correlation function can be expressed as the fourier transform of delay power spectrum density function, the time-frequency correlation function is derived as follow:

$$R^{NLOS}(\tau, f) = \int S_h(\tau, \xi) \exp(-j2\pi f \xi) d\xi = \frac{\Omega^{-1}}{1+K_{Rice}} \iiint f(\phi|\tau)f(\tau) (d_{tk} \times d_{kr})^{-w_{pathloss}} \times \exp[-j\frac{2\pi}{\lambda} \xi c - j2\pi f \xi_k] \delta(\xi - \xi_k) d\phi d\tau d\xi \quad (17)$$

#### 4. The simulation

In order to prove the feasibility and applicability of the 3D-MIMO-GBSBEM proposed in this study, MATLAB simulation is utilized. In this study's preliminary experiment, we set  $d_0 = 500m$ ,  $\sigma = 5\mu s$ . Assuming a MIMO channel bandwidth of the input signal is 1MHz. The coefficients of cross-correlation function are obtained by AR model. The channel simulation is achieved by tapped delay line model. The number of taps is 5, and the order of AR model is 50.

In Fig. 4, we show the AOA's PDFs of the GBSBEM and the improved 3D-GBSBEM model in different pitch angle cases. Seen from Fig. 4, the improved AOA's PDF has the same distribution with the GBSBEM, when the pitch angle is zero, i.e. the transmitting antenna and the receiving antenna is located in the same horizontal plane. And the values mostly concentrate in the small angle region. When there is a smaller pitch angle ( $\phi < \pi/2$ ) between the

receiving antenna and the transmitting antenna, the distribution of PDF becomes flat.

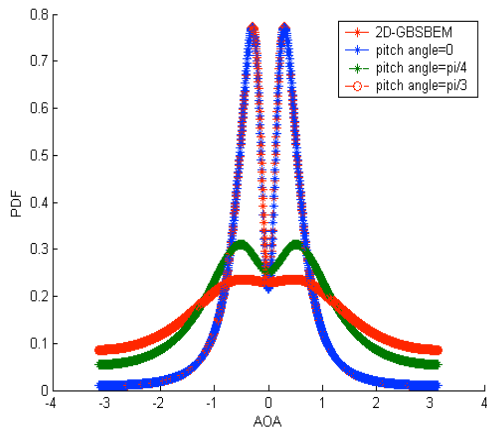


Fig. 4. the PDF of AOA for 3D-GBSBEM

In Fig. 5, we show the relationship between the improved AOA distribution and the time delay in the case of same pitch angle. Seen from Fig. 5, the angle of arrival is mainly distributed in a region with small delay. As the time delay increases, the distribution of the AOA gradually spread.

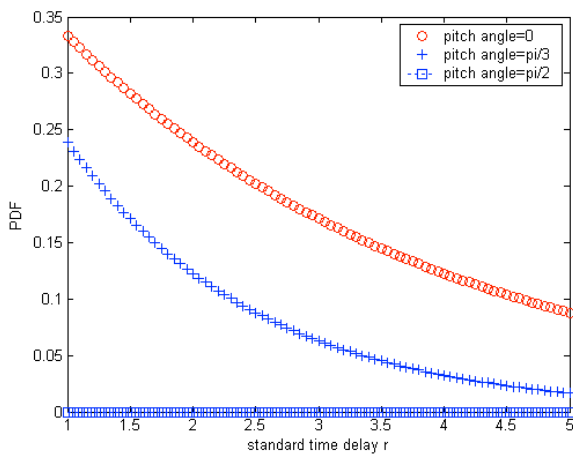


Fig. 5. The PDF of standard time delay for 3D-GBSBEM

In order to verify the performance of the 3D-MIMO-GBSBEM model under frequency selective environment, this paper simulated the model's delay profile, and compare the delay profile with the measurement results in literature [7]. Literature [7] measured the delay profile under the condition of low base station antennas. In order to approximate the measured environment, the simulation parameter defined as:

$$W_{pathloss} = 2.25, D=1000m, \theta = 15^\circ$$

The delay profile simulation result is shown in Fig.6. It can be seen from Fig.6 that the delay profile of 3D-MIMO-GBSBEM simulated in MATLAB is consistent with the measurement results of Literature [7]. It means that the 3D-MIMO-GBSBEM can accurately describe the characteristics of the frequency selective multipath fading channel.

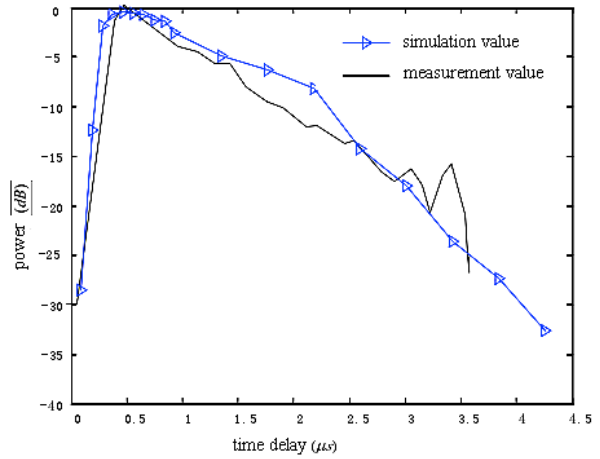


Fig. 6. the delay profile for 3D-MIMO-GBSBEM

To the  $2 \times 2$  antenna element for example, this paper simulated the space time correlation function ( $R(\tau)$ ) of 3D-MIMO-GBSBEM. The simulation parameter defined as: carrier frequency ( $f_c$ ) is 2GHz, height of transmitting antennas is  $h_p = h_q = 10\lambda$ , and the height of receiving antennas is  $h_m = h_n = 5\lambda$ . The distance between transmitting antenna and receiving antennas is 1000m. In Fig. 7, we show the comparison between the correlation value of 3D-MIMO-GBSBEM obtained by theoretical analysis and the related characteristics obtained by simulation. L is the number of paths. It can be seen that, the greater of L, the more similar the theoretical curve and the simulation curve.

It can be seen from the simulation of 3D-GBSBEM, there is a close relationship among the time delay, arrival angle and spatial distance between transmitting antennas and receiving antennas. For a receiver, the reception will be better, if the time delay is smaller and the concentration of AOA is higher. Therefore a suitable compromise between the height and distance of the receiver is needed.

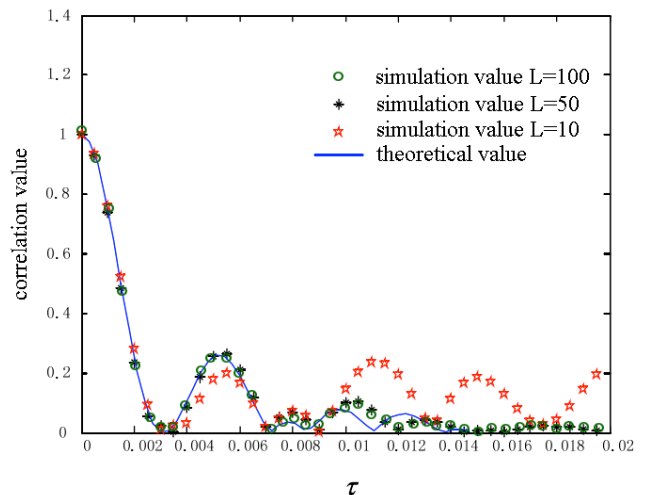


Fig. 7. The space time correlation function for 3D-MIMO-GBSBEM

In addition, the delay profile and space time correlation function of 3D-MIMO-GBSBEM can more accurately describe the frequency-selective multipath fading channel correlation properties compared with measurement.

Therefore, this improved model can provide a theoretical basis for the performance analysis of receiver to achieve optimum reception.

## 5. Conclusion

This study analyzes the limitations of traditional GBSBEM, and proposes an improvement 3D-MIMO-GBSBEM. The probability density function of the angle of arrived, space time frequency correlation function, and delay power spectrum density function are derived. Compared with the traditional GBSBEM, this improved model has the following characteristics:

(1) There is a degree of freedom to describe the cellular space environment. Selecting appropriate characterization of

the transceiver antenna space distance, the model is applied to city buildings and rural communication environment.

(2) It is more intuitive and reasonable to explain the physical characteristics of wireless fading propagation. The simulation results show that the traditional GBSBEM can be regarded as a subset of the improved model in the ideal environment. The proposed model is not only compatible with the traditional GBSBEM, but also effective to overcome the limitations of the latter to make the model more suitable for the actual environment needs.

---

## References

1. *Liberti J C, Rappaport T S.*, "A geometrically based model for line-of-sight multipath radio Channels", IEEE 46th Vehicular Technology Conference[C]. Atlanta: IEEE, 1996, pp.844-848.
2. *Ertel R B, Reed J H.*, "Angle and time of arrival statistics for circular and elliptical scattering models", IEEE Journal on Selected Areas in Communications, 17(11), 1999, pp.1829-1840.
3. *Lee. W C Y.*, "Mobile Communications Engineering", New York: McGraw Hill Publications, 1982.
4. *Aszetyl D (1996).* "On Antenna Array in Mobile Communication Systems: Fast fading and GSM Base Station Receiver Algorithm", Royal Instituted of Technology Ph.D.
5. *Lee W C Y, Brandt R H.*, "The elevation angle of mobile radio signal arrival", IEEE Transactions on Communications, 21, pp.1194-1197.
6. *Leong S-Y, Zheng Y R, Xiao C.*, "Space-time fading correlation functions of a 3-DMIMO channel Model", In: 2004 IEEE Wireless Communications and Networking Conference, 2004. WCNC, pp.1127-1132.
7. *Yong S K, Thompson J S.*, "Three-dimensional spatial fading correlation models for compact MIMO receivers", Wireless Communications, IEEE Transactions, 4(6) ,2005, pp.2856-2869.
8. *Yong S K, Thompson J S.*, "A three-dimensional spatial fading correlation model for uniform rectangular arrays", IEEE Antennas and Wireless Propagation Letters, 2, 2003. pp. 182-185.
9. *Mala Umar Mustapha Bakura.*, "Geometrically based MIMO mobile-to-mobile channel model", Beijing: Beijing University of Posts and Telecommunications, 2013(01), pp. 89-91.
10. *B. S. Reddy, N. J. Krishna, J.S. Kumar and K.V.K. Reddy.*, "Prediction of Surface Roughness in End Milling of P20 Mould Steel Using Artificial Neural Networks", 5(1), 2012, pp.7-13.
11. *Sh. Mirseidova, A. Inoue, L. Atymtayeva.*, "Evaluation of Fair Market Price of Resources In Oil And Gas Industry Using Fuzzy Sets And Logics", 16(1), 2012, pp.30-34.